An Artificial Protein Cage Made from a 12-Membered Ring

Electronic Supplementary Information (ESI)

Izabela Stupka[1,2,#], Artur P. Biela[1,3*], Bernard Piette[4], Agnieszka Kowalczyk[1,5], Karolina Majsterkiewicz[1,2], Kinga Borzęcka-Solarz[1], Antonina Naskalska[1], Jonathan G. Heddle[1$ *]

[1] Malopolska Centre of Biotechnology, Jagiellonian University, Krakow, Poland

[2] Postgraduate School of Molecular Medicine, Warsaw, Poland

[3] Institute of Zoology and Biomedical Research, Jagiellonian University, Krakow, Poland

[4] Department of Mathematical Sciences, Durham University, Durham, UK

[5] Faculty of Mathematics and Computer Science, Jagiellonian University, Krakow, Poland

[#]Current address: nCage Therapeutics, Krakow, Poland

[$]Current address: Department of Biosciences, Durham University, Durham, UK

* To whom correspondence should be addressed. artur.biela@uj.edu.pl, jonathan.g.heddle@durham.ac.uk

Table of Contents

Supplementary Tables

Table S1. Comparison of the stability of $^{11}TRAP_{24}$, $^{11}TRAP_{12}$ and $^{12}TRAP_{12}$-cages

	$^{11}TRAP_{24}$*	$^{11}TRAP_{12}$**	$^{12}TRAP_{12}$
Temperature (°C), 10 min	>120	70	80
pH range	3-12	4-11	5-10
Urea (M)	>7	3	3
Gnd-HCl (M)	4	2	1
SDS (%)	>3	>3	<0.05
DTT (mM)	0.7	0.7	1
TCEP (mM)	0.07	0.07	0.01
Glutathione, reduced (mM)	0.7	0.7	1
Glutathione, oxidized (mM)	>70	>70	>10

* - values from[1]

** - values from[2]

name of the structure	#faces and their polygonality	underlying topological structure (symmetry)	Δ_l	Δ_α	dihedral α	types and number of holes		chirality	equivalent faces; #adjacent faces	#bonds; saturated faces	structure diameter to face diameter ratio
Aco_P10_1_2_1_2 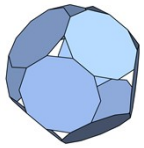	12x10-gons	cuboctahedron	0.001%	0.51%	120°	8 triangular, 6 four-fold		no	yes; 4	48; no	1.914
Pic_P10_1_1_1_1_1 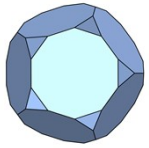	12x10-gons	icosahedron	0%	0%	116.565°	20 triangular		no	yes; 5	60; yes	1.835
Aco_P11_1_2_1_3 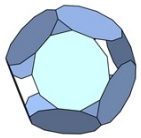	12x11-gons	cuboctahedron	1.76%	1.806%	119.393°	8 triangular, 6 bowtie		no	yes; 4	48; no	1.916
Aco_P13_2_2_2_3 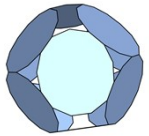	12x13-gons	cuboctahedron	2.698%	2.698%	119.46°	8 tripod-like, 6 bowtie		no	yes; 4	48; no	1.862
Pic_P13_1_2_1_2_2 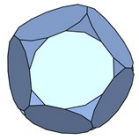	12x13-gons	icosahedron	5.61%	5.611%	120.572° (between faces adjacent to two tripod-like holes) 115.499° (all the other)	8 triangular, 12 tripod-like		no	yes; 5	60; no	1.782

Table S2. A selection of results of theoretical protein cages produced from TRAP rings containing different numbers of monomers

Table S3. A selection of results of theoretical protein cages produced from TRAP rings containing 12 monomers

name of the structure	#faces and their polygonality	underlying topological structure (symmetry)	Δ_l	Δ_α	dihedral α	types and number of holes	chirality	equivalent faces; #adjacent faces	#bonds; saturated faces	structure diameter to face diameter ratio
Aco_P12_1_2_1_4 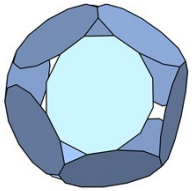	12x12-gons	cuboctahedron	3.805%	3.805%	117.875°	8 triangular, 6 bowtie	no	yes; 4	48; no	1.842
Aco_P12_1_3_1_3 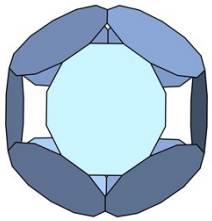	12x12-gons	cuboctahedron	0%	1,7%	120°	8 triangular, 6 bowtie	no	Yes; 4	48; no	1.901
Pic_P12_2_1_2_1_1 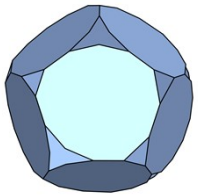	12x12-gons	icosahedron	6.157%	6.157%	111.836° (between faces adjacent to two small triangular holes) 117.654° (all the other)	12 triangular, 8 tripod-like	no	yes; 5	60; no	1.906

Table S2 and S3 Notes

Name of the structure - a notation is made out of three parts SYM_PN_QI, where PN is the letter P followed by the number of edges of the cage faces; SYM refers to the underlying topological structure (Pic for Platonic icosahedron, Aco for Archimedean cuboctahedron) from which the cage is constructed; QI refers to the sequence of edges (separated by the symbol '_') that each face contributes to the adjacent holes. More details can be found in[3].

Relative errors Δ_l (for edge lengths), Δ_α (for face planar angles) – deviations from regularity are expressed as relative deformations and defined as the largest absolute value of the difference between the edge lengths (angles) and the average edge length (angle), divided by the average value. More details can be found in[3,4].

Equivalent faces - every face can be mapped onto any other face by means of proper rotations; every face "is the same". More details can be found in[3,4] .

#bonds – number of glued edges between the faces x 2; number of chemical bonds that can be present in an actual cage

Saturated faces – faces that are adjacent to the maximal number of other faces of the same type under the condition that no two consecutive face edges are glued to another face or faces.

Structure diameter to face diameter ratio – ration between the diameter of the structure to the diameter of the regular face.

Table S4. Discarded models. Table includes an explanation of why some cages deemed invalid and not included in the shortlist of likely cages (as shown in Table S1)

#	name of the structure	underlying topological structure (symmetry)	Δ_l	Δ_α	dihedral α	types and number of holes	chirality	equivalent faces; #adjacent faces	#bonds; saturated faces	structure diameter to face diameter ratio	comment
12x10-gons											
1	**Att_P10_1_3_3**	truncated tetrahedron	0%	0%	63.4°(between faces adjacent to a triangular hole), 145.3° (all the other)	4 triangular, 4 three-fold (between six faces)	no	yes; 3	36; no	2.377	too large 3-fold holes
2	**hp_P10_3_2_2**	hexagonal prism	0%	0%	131.2° (between faces adjacent to a six-fold hole), 111.5° (all the other)	6 two-fold, 2 six-fold	no	yes; 3	36; no	2.288	too large 6-fold holes
3	**Att_P10_1_2_4**	truncated tetrahedron	1.33%	1.33%	126.288°(between faces adjacent to a triangular hole), 127.225°(all the other)	4 triangular, 4 three-fold (between six faces)	yes	yes; 3	36; no	2.126	too large 3-fold holes
4	**ha_P10_3_1_1_1**	hexagonal antiprism	4.357%	4.358%	126. 817-126.831° (between faces adjacent to a six-fold hole), 119.68-119.69° (all the other)	12 triangular holes, 2 six-fold	no	yes; 4	48; no	2.127	too large 6-fold holes
5	**hp_P10_3_1_3**	hexagonal prism	4.731%	3.435%	125.931- 125.934° (between faces adjacent to a six-fold hole), 122.516- 122.518° (all the other)	6 two-fold (they seem to be 12 triangular holes but are not), 2 six-fold	yes	yes; 3	36; no	2.084	too large 6-fold holes
6	**hp_P10_2_2_3**	hexagonal prism	8.02%	8.02%	160.738- 160.741°(between faces adjacent to a six-fold hole), 38.864° (all the other)	6 two-fold, 2 six-fold	yes	yes; 3	36; no	2.636	too large 6-fold holes, too flat structure globally
12x11-gons											
1	**hp_P11_4_2_2**	hexagonal prism	0%	0%	57.9°(between faces adjacent to a six-fold hole), 151.2° (all the other)	6 two-fold, 2 six-fold	no	yes; 3	36; no	2.403	too large 6-fold holes
2	**Att_P11_1_3_4**	truncated tetrahedron	0.508%	0.508%	130.842- 130.846°(between faces adjacent to a triangular hole), 126.749- 126.753°(all the other)	4 triangular, 4 three-fold (between six faces)	yes	yes; 3	36; no	2.280	too large 3-fold holes
3	**Aco_P11_1_2_2_2**	cuboctahedron	0.041%	1.493%	84.44-84.46° (between faces	4 triangular, 6 two-	no	yes; 4	48; no	2.280	not

					adjacent to a three-fold hole), other in the range of 159.65-159.67°	fold, 4 three-fold					spherical in shape enough, too flat locally
4	**Att_P11_1_2_5**	truncated tetrahedron	1.176%	1.176%	all in the range of 124.181-124.243 °	4 triangular, 4 three-fold (between six faces)	yes	yes; 3	36; no	2.087	less bonds between the faces in comparison with **Aco_P11_1_2_1_3**
5	**Att_P11_2_3_3**	truncated tetrahedron	2.5%	2.502%	88.655- 91.25 ° (between faces adjacent to a star-shaped hole), 179.99-180° (all the other)	4 three-fold star-shaped between 3 faces, 4 three-fold between six faces	no	yes; 3	36; no	2.497	too large 3-fold holes
6	**hp_P11_4_1_3**	hexagonal prism	3.237%	3.237%	124.815- 124.819°(between faces adjacent to a six-fold hole), 127.337° (all the other)	6 two-fold (they seem to be 12 triangular holes but are not), 2 six-fold	yes	yes; 3	36; no	2.117	too large 6-fold holes
7	**ha_P11_4_1_1_1**	hexagonal antiprism	4.179%	4.178%	124.828°(between faces adjacent to a six-fold hole), 126.914°(all the other)	12 triangular holes, 2 six-fold	no	yes; 4	48; no	2.104	too large 6-fold holes
8	**hp_P11_3_2_3**	hexagonal prism	4.826%	4.827%	138.917- 138.924°(between faces adjacent to a six-fold hole), 88.362- 88.363°(all the other)	6 two-fold, 2 six-fold	yes	yes; 3	36; no	2.451	too large 6-fold holes, too flat structure globally
9	**Att_P11_2_1_5**	truncated tetrahedron	7.479%	7.479%	121.294-121.3° (between faces adjacent to a star-shaped hole), 114.378- 114.383° (all the other)	4 three-fold star-shaped, 4 three-fold (between six faces)	yes	yes; 3	36; no	1.811	much larger deformation than in **Aco_P11_1_2_1_3**
10	**hp_P11_2_3_3**	hexagonal prism	7.647%	7.647%	154.244- 154.248°(between faces adjacent to a six-fold hole), 52.938- 52.939° (all the other)	6 two-fold, 2 six-fold	no	yes; 3	36; no	2.597	too large 6-fold holes, too flat structure globally + much larger deformation than in

											Aco_P11_1_2_1_3
11	**Aco_P11_2_1_2_2**	cuboctahedron	8.688%	8.69%	all in the range of 119.166-119.173 °	8 three-fold, 6 bowtie	no	yes; 4	48; no	1.757	much larger deformation than in **Aco_P11_1_2_1_3**
12	**Att_P11_2_2_4**	truncated tetrahedron	9.01%	9.011%	125.081- 125.122° (between faces adjacent to a star-shaped hole), 129.453- 129.491° (all the other)	4 three-fold star-shaped hole between 3 faces, 4 three-fold between six faces	yes	yes; 3	36; no	2.042	much larger deformation than in **Aco_P11_1_2_1_3**
13	**Aco_P11_1_1_2_3**	cuboctahedron	9.391%	9.391%	118.059°(between faces adjacent to a three-fold hole), 116.453°(all the other)	4 triangular, 4 three-fold, 6 two-fold (they seem to be 12 triangular holes but are not)	no	yes; 4	48; no	1.817	much larger deformation than in **Aco_P11_1_2_1_3**
12x12-gons											
1	**Att_P12_1_4_4**	truncated tetrahedron	0%	0%	180° between faces adjacent to a triangular hole, 70.52° (all the other)	4 triangular, 4 three-fold (between six faces)	no	yes; 3	36; no	2.551	too large 3-fold holes, too flat locally
2	**Aco_P12_1_2_3_2**	cuboctahedron	0%	0%	180° between faces adjacent to a triangular hole, 70.52° (all the other)	4 triangular, 6 two-fold, 4 three-fold	no	yes; 4	48; no	2.358	not spherical in shape enough, too flat locally
3	**hp_P12_5_2_2**	hexagonal prism	0%	0%	60°(between faces adjacent to a six-fold hole), 180° (all the other)	6 two-fold, 2 six-fold	no	yes; 3	36; no	2.579	too large 6-fold holes, too flat locally
4	**hp_P12_3_3_3**	hexagonal prism	0%	0%	180° (between faces adjacent to a six-fold hole), all the other 0°	6 two-fold, 2 six-fold	no	yes; 3	36; no	2.903	globally flat structure
5	**hp_P12_4_2_3**	hexagonal prism	0.401%	0.401%	127.079°(between faces adjacent to a six-fold hole), 124.511° (all the other)	6 two-fold, 2 six-fold	yes	yes; 3	36; no	2.178	too large 6-fold holes
7	**Aco_P12_2_2_2_2**	cuboctahedron	0.001%	4.326%	all in the range of 119.998-120.002°	8 three-fold, 6 four-fold	no	yes; 4	48; no	1.906	too large 3-fold holes
8	**Att_P12_1_3_5**	truncated	2.316%	2.317%	130.077- 130.091° (between	4 triangular, 4 three-	yes	yes; 3	36; no	2.214	too large 3-

		tetrahedron			faces adjacent to a triangular hole), 124.858- 124.878° (all the other)	fold (between six faces)					fold holes
9	**Att_P12_2_2_5**	truncated tetrahedron	5.804%	5.804%	126.133- 126.141°(between faces adjacent to a star-shaped hole), 123.42- 123.43° (all the other)	4 three-fold star-shaped hole between 3 faces, 4 three-fold between six faces	yes	yes; 3	36; no	2.004	less bonds between the faces and larger deformation in comparison with **Aco_P12_1_2_1_4**
10	**Aco_P12_2_1_2_3**	cuboctahedron	4.266%	6.357%	all in the range of 117.742- 117.744°	8 three-fold, 6 two-fold (they seem to be 12 triangular holes but are not)	no	yes; 4	48; no	1.900	larger deformation than **Aco_P12_1_2_1_4**
11	**Aco_P12_1_2_2_3**	cuboctahedron	6.439%	6.439%	95.60- 95.61° (between faces adjacent to a three-fold hole), 145.391- 145.396° (all the other)	4 triangular, 6 two-fold, 4 three-fold	yes	yes; 4	48; no	2.079	larger deformation than **Aco_P12_1_2_1_4** and **Pic_P12_2_1_2_1_1**
12	**Att_P12_2_3_4**	truncated tetrahedron	6.895%	6.901%	101.322- 101.341°(between faces adjacent to a star-shaped hole), 164.15- 164.174° (all the other)	4 three-fold star-shaped hole between 3 faces, 4 three-fold between six faces	yes	yes; 3	36; no	2.297	larger deformation than **Aco_P12_1_2_1_4** and **Pic_P12_2_1_2_1_1**
13	**Att_P12_3_3_3**	truncated tetrahedron	8.017%	8.29%	89.572- 90.391°(between faces adjacent to a star-shaped hole), 179.991- 179.994° (all the other)	4 three-fold star-shaped hole between 3 faces, 4 three-fold between six faces	no	yes; 3	36; no	2.300	larger deformation than **Aco_P12_1_2_1_4** and **Pic_P12_2_**

											1_2_1_1
14	**hp_P12_5_1_3**	hexagonal prism	8.236%	8.235%	124.179- 124.195°(between faces adjacent to a six-fold hole), 130.495- 130.498° (all the other)	6 two-fold (they seem to be 12 triangular holes but are not), 2 six-fold	yes	yes; 3	36; no	2.112	too large 6-fold holes, larger deformation than **Aco_P12_1_2_1_4** and **Pic_P12_2_1_2_1_1**
15	**hp_P12_3_2_4**	hexagonal prism	9.466%	9.466%	142.274- 142.28°(between faces adjacent to a six-fold hole), 78.769- 78.771° (all the other)	6 two-fold, 2 six-fold	yes	yes; 3	36; no	2.429	too large 6-fold holes, too flat structure globally; larger deformation than **Aco_P12_1_2_1_4** and **Pic_P12_2_1_2_1_1**
12x13-gons											
1	**Att_P13_2_4_4**	truncated tetrahedron	0%	0%	82.1° (between faces adjacent to a star-shaped hole), 169.2° (all the other)	4 three-fold star-shaped hole between 3 faces, 4 three-fold between six faces	no	yes; 3	36; no	2.566	too large 3-fold holes, too flat locally
2	**hp_P13_4_3_3**	hexagonal prism	0%	0%	135.7° (between faces adjacent to a six-fold hole), 82.1° (all the other)	6 two-fold, 2 six-fold	no	yes; 3	36; no	2.466	too large 6-fold holes
3	**Aco_P13_1_3_2_3**	cuboctahedron	0.021%	2.357%	93.359- 93.372° (between faces adjacent to a star-shaped hole), 148.707- 148.724° (all the other)	4 triangular, 6 two-fold, 4 three-fold star-shaped	no	yes; 4	48; no	2.204	less spherical in shape than **Aco_P13_2_2_2_3** and **Aco_P13_2_**

											2_2_3 can be optimized to get similar distortion to this structure
4	**Att_P13_1_4_5**	truncated tetrahedron	2.404%	2.414%	147.885- 148.119° (between faces adjacent to a triangular hole), 107.064- 107.272° (all the other)	4 triangular, 4 three-fold (between six faces)	yes	yes; 3	36; no	2.415	too large 3-fold holes
5	**Att_P13_2_2_6**	truncated tetrahedron	3.351%	3.35%	123.559- 123.563°(between faces adjacent to a star-shaped hole), 120.866- 120.871° (all the other)	4 three-fold star-shaped hole between 3 faces, 4 three-fold between six faces	yes	yes; 3	36; no	1.985	less bonds between the faces and larger deformation in comparison with **Aco_P13_2_2_2_3**
6	**Aco_P13_2_2_3_2**	cuboctahedron	2.583%	5.066%	79.078- 79.082° (between faces adjacent to a two-fold hole), 166.852- 166.859° (all the other)	8 three-fold (two groups of 4 of different shape), 6 two-fold	no	yes; 4	48; no	2.161	too flat locally, larger angle deformation than **Aco_P13_2_2_2_3**
7	**hp_P13_4_2_4**	hexagonal prism	3.994%	3.994%	128.758- 128.761°(between faces adjacent to a six-fold hole), 115.485° (all the other)	6 two-fold, 2 six-fold	yes	yes; 3	36; no	2.201	too large 6-fold holes
8	**hp_P13_5_2_3**	hexagonal prism	4.004%	4.004%	123.309- 123.424°(between faces adjacent to a six-fold hole), 141.686- 141.696 ° (all the other)	6 two-fold, 2 six-fold	yes	yes; 3	36; no	2.290	too large 6-fold holes
9	**Att_P13_1_3_6**	truncated tetrahedron	4.082%	4.082%	127.355- 127.365° (between faces adjacent to a triangular hole), 124.276- 124.292° (all the other)	4 triangular, 4 three-fold (between six faces)	yes	yes; 3	36; no	2.146	less bonds between the faces and larger deformation

											in comparison with **Aco_P13_2_2_2_3**
10	**Att_P13_2_3_5**	truncated tetrahedron	4.212%	4.211%	124.078- 124.087°(between faces adjacent to a star-shaped hole), 132.415- 132.425° (all the other)	4 three-fold star-shaped hole between 3 faces, 4 three-fold between six faces	yes	yes; 3	36; no	2.160	less bonds between the faces and larger deformation in comparison with **Aco_P13_2_2_2_3** + too large 3-fold holes
11	**Aco_P13_1_3_1_4**	cuboctahedron	4.229%	5.013%	all in the range of 119.674- 119.694°	8 triangular, 6 bowtie	no	yes; 4	48; no	1.879	larger deformation than **Aco_P13_2_2_2_3**
12	**hp_P13_3_3_4**	hexagonal prism	5.273%	5.271%	162.21- 162.394°(between faces adjacent to a six-fold hole), 35.674-35.702° (all the other)	6 two-fold, 2 six-fold	yes	yes; 3	36; no	2.748	too large 6-fold holes, too flat structure globally
13	**Aco_P13_1_2_2_4**	cuboctahedron	6.163%	6.163%	112.223°(between faces adjacent to a star-shaped hole), 123.98° (all the other)	4 triangular, 6 bowtie, 4 three-fold star shaped	yes	yes; 4	48; no	1.945	larger deformation than **Aco_P13_2_2_2_3** and **Pic_P13_1_2_1_2_2**
14	**hp_P13_6_2_2**	hexagonal prism	6.252%	6.247%	118.816- 120.762°(between faces adjacent to a six-fold hole), 179.997° (all the other)	6 two-fold, 2 six-fold	no	yes; 3	36; no	2.480	too large 6-fold holes, too flat locally
15	**Aco_P13_1_2_4_2**	cuboctahedron	7.239%	7.283%	70.71- 71.12°(between faces adjacent to a star-shaped hole), 179.356- 179.459° (all	4 triangular, 6 two-fold, 4 three-fold star-shaped	no	yes; 4	48; no	2.204	too flat locally, larger

					the other)						deformation than **Aco_P13_2_2_2_3** and **Pic_P13_1_2_1_2_2**
16	**Aco_P13_1_2_3_3**	cuboctahedron	8.885%	8.887%	75.38- 75.385°(between faces adjacent to a star-shaped hole), 172.036- 172.041° (all the other)	4 triangular, 6 two-fold, 4 three-fold star-shaped	yes	yes; 4	48; no	2.195	too flat locally, larger deformation than **Aco_P13_2_2_2_3** and **Pic_P13_1_2_1_2_2**

Table S5. Plasmids and amino acid sequences

Plasmid name	Plasmid	Gene	Amino acid sequence
pET21b_TRAP-K37C	pET21b	12-mer-TRAP-K37C	MNVGDNSNFFVIKAKENGVNVFGMTRGTDTRFHHSECLDKGEVMIAQFTEHTSAVKIRGKAIIQTSYGTLDTEKDE
pET21b_12-merTRAP-wt	pET21b	12-mer-TRAP-wt	MNVGDNSNFFVIKAKENGVNVFGMTRGTDTRFHHSEKLDKGEVMIAQFTEHTSAVKIRGKAIIQTSYGTLDTEKDE
pET21b_11-merTRAP-K35C-R64S	pET21b	11-mer-TRAP-K35C-R64S	MYTNSDFVVIKALEDGVNVIGLTRGADTRFHHSECLDKGEVLIAQFTEHTSAIKVRGKAYIQTSHGVIESEGKK

Table S6. Cryo-EM data collection statistics

	$^{12}TRAP_{12}$	$^{11}TRAP_{12}$
EMDB	17196	17195
Data collection and processing		
Magnification	165k	175k
Voltage (kV)	300	300
Electron exposure (e–/Å^2)	40	40
Defocus range (μm)	0.5-2.5	0.8-2.4
Pixel size (Å)	1.065	0.86
Symmetry imposed	T	T
Initial particle images (no.)	848,602	1.479,225
Final particle images (no.)	143,338	406,311
Map resolution (Å)	7.00	4.68
FSC = 0.143		

Supplementary Movie 1.

3D variability of the $^{12}TRAP_{12}$ cage showing its flexible nature. The movie is composed from 20 different states (frames representing least scattered clusters) being a result of 3D variability analysis (3DVA) morphed sequentially one into another using ChimeraX giving the impression of a "breathing" cage. All densities (frames) are contoured at the same RMSD level of 3.5.

References

1 A. D. Malay, N. Miyazaki, A. Biela, S. Chakraborti, K. Majsterkiewicz, I. Stupka, C. S. Kaplan, A. Kowalczyk, B. M. A. G. Piette, G. K. A. Hochberg, D. Wu, T. P. Wrobel, A. Fineberg, M. S. Kushwah, M. Kelemen, P. Vavpetič, P. Pelicon, P. Kukura, J. L. P. Benesch, K. Iwasaki and J. G. Heddle, *Nature*, 2019, **569**, 438–442.

2 K. Majsterkiewicz, A. P. Biela, S. Maity, M. Sharma, B. M. A. G. Piette, A. Kowalczyk, S. Gaweł, S. Chakraborti, W. H. Roos and J. G. Heddle, *Nano Lett.*, 2022, **22**, 3187–3195.

3 B. M. A. G. Piette, A. Kowalczyk and J. G. Heddle, *Proc. R. Soc. A Math. Phys. Eng. Sci.*, 2022, **478**, 20210679.

4 J. G. Heddle, A. Kowalczyk and B. M. A. G. Piette, in *Bridges 2019 Conference Proceedings*, Tessellations Publishing, Phoenix, Arizona, 2019, pp. 363–366.

Supplementary Figures

a)

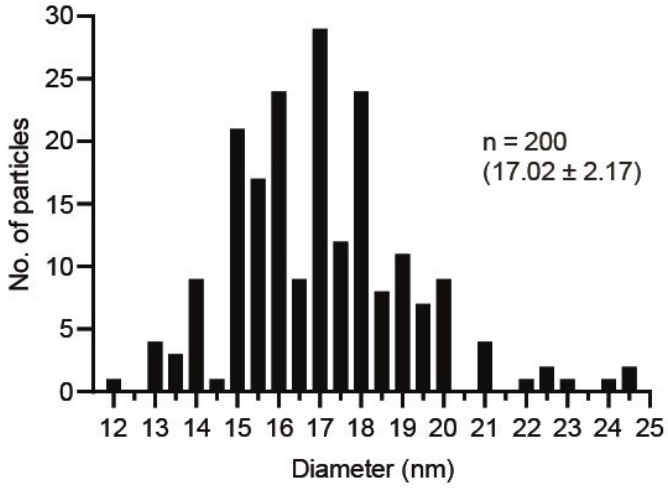

Diameter range (nm)	<15	15-18	>18
Number of particles	18	136	46
(%)	9	68	23

b)

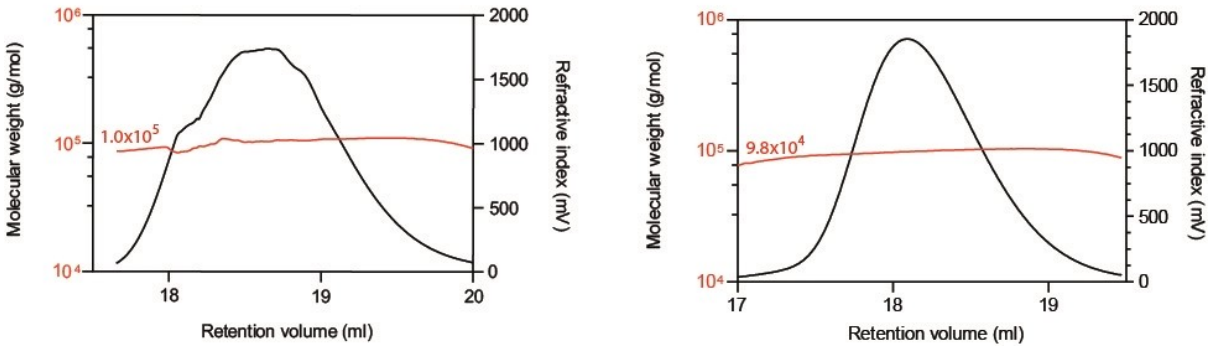

Fig. S1. Confirmation of ^{12}TRAP –cage formation (a), Analysis of 200 particles from an electron micrograph of ^{12}TRAP-cage (same sample as in Fig. 3a) indicating a mean diameter of approx. 17 nm. **(b), control showing effect of Au(I)-TPPMS on wild type** ^{12}TRAP-rings. Typical Refractive Index (RI) chromatogram of ^{12}TRAP-rings(wt) before (left) and after (right) addition of Au(I)-TPPMS with indicated measured molecular weight.

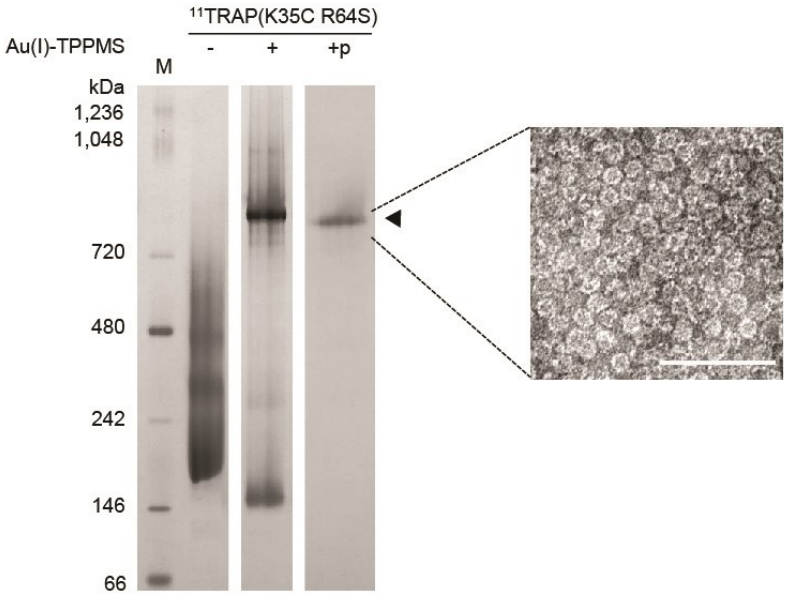

Fig. S2. Confirmation of $^{11}TRAP_{12}$ formation. Dark Blue Native PAGE of 11TRAP-K35C R64S rings before and after the addition of Au(I)-TPPMS. 'p' indicates the purified sample. 'M' denotes molecular mass marker. Position of $^{11}TRAP_{12}$ is indicated by black arrowhead. Inset: Transmission electron microscopy (TEM) image of $^{11}TRAP_{12}$. Scale bar, 100 nm.

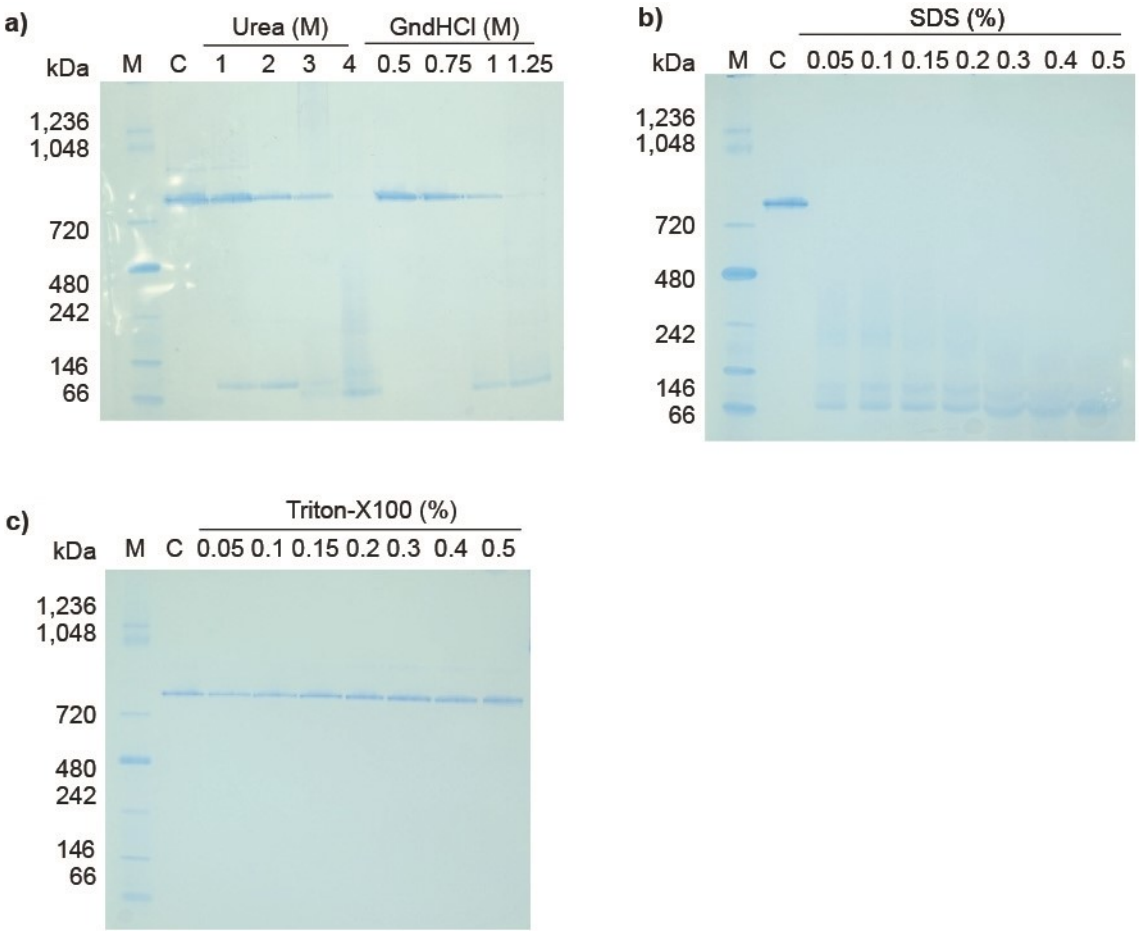

Fig. S3. Stability of ^{12}TRAP–cage. Native PAGE analysis of ^{12}TRAP-cage stability in the presence of urea, guanidine hydrochloride (GndHCl) **(a)**, SDS **(b)** and Triton X-100 **(c)**. "C" denotes ^{12}TRAP-cage. "M", molecular weight marker.

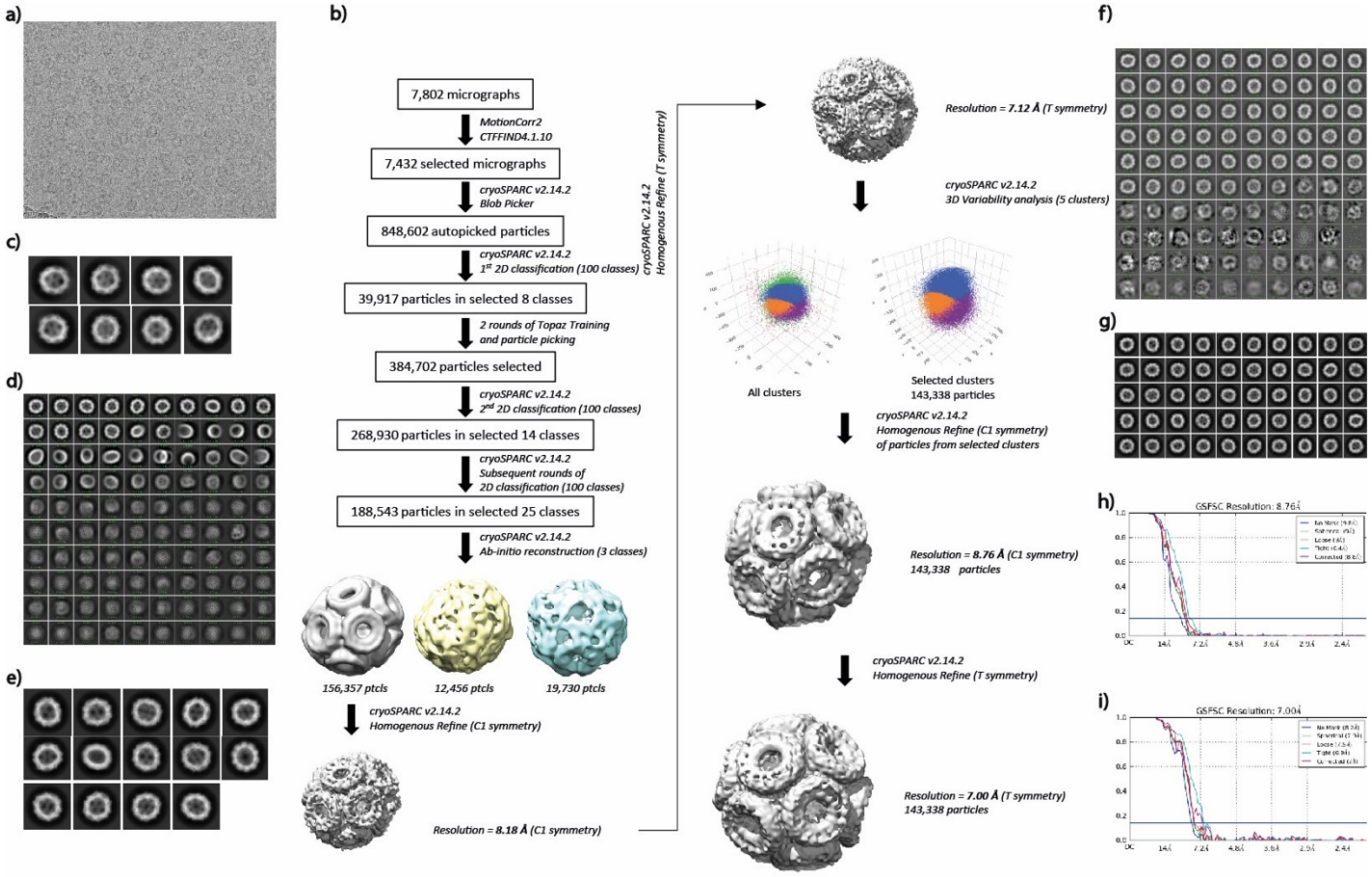

Fig. S4. Procedure for cryo-EM reconstruction of Au-TPPMS 12-mer TRAP cage. (a), representative micrograph. Scale bar – 50 nm. (**b),** Summary of the image processing procedure (see Methods). **(c),** selected 2D class averages from first reference-free 2D classification in cryoSPARC v2.14.2 used to train Topaz[19,20] (**d),** 2D class averages from reference-free 2D classification in cryoSPARC v2.14.2. **(e),** first selected twelve 2D classes. **(f),** final 2D class averages from reference-free 2D classification in cryoSPARC v.2.14.2. (**g),** Final 2D classes selected for 3D reconstruction. **(h),** FSC correlation curve for structure refined in C1 symmetry. (**i),** FSC correlation curve for structure refined in tetrahedral symmetry (T).

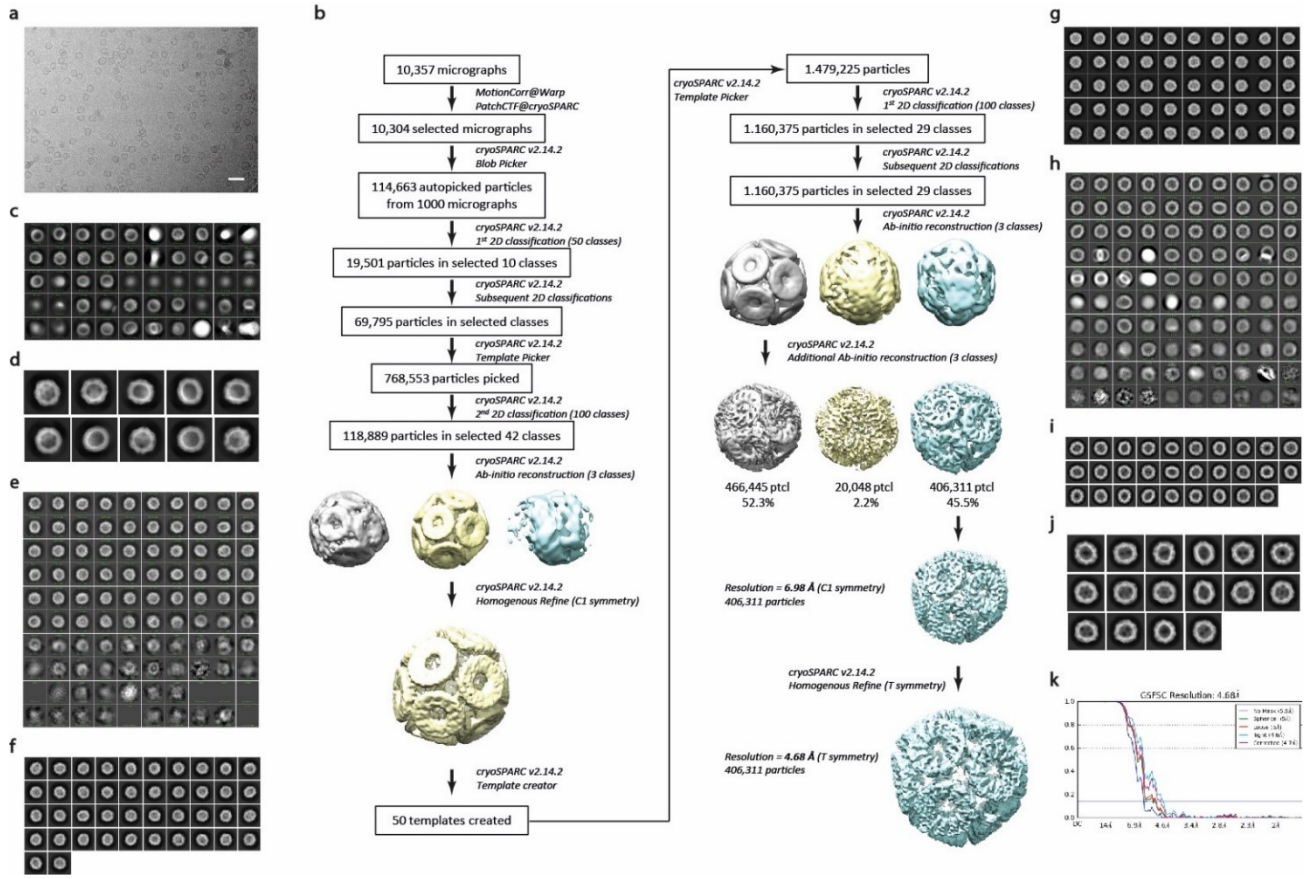

Fig. S5. Procedure for cryo-EM reconstruction of Au-TPPMS $^{11}TRAP_{12}$. (a), representative micrograph. Scale bar – 50 nm. (**b),** Summary of the image processing procedure (see Methods). (**c),** results of the first 2D classification. (**d),** selected 2D class averages from first reference-free 2D classification in cryoSPARC v2.14.2 used for 1st template pick **(e),** 2D class averages from reference-free 2D classification in cryoSPARC v2.14.2. after 1st template pick (**f),** 2D classes selected for the 1st Ab-initio reconstruction. (**g),** 50 back projections created from initial 3D volume. **(h),** result of the 2D classification after template picking from back-projection-create 2D classes. **(i),** the first selection of 2D classes. **(j),** final 2D classes used for generation of a 3D map. **(k),** FSC curve with indicated resolution at 0.143 thresholds for the final refinement in T symmetry.

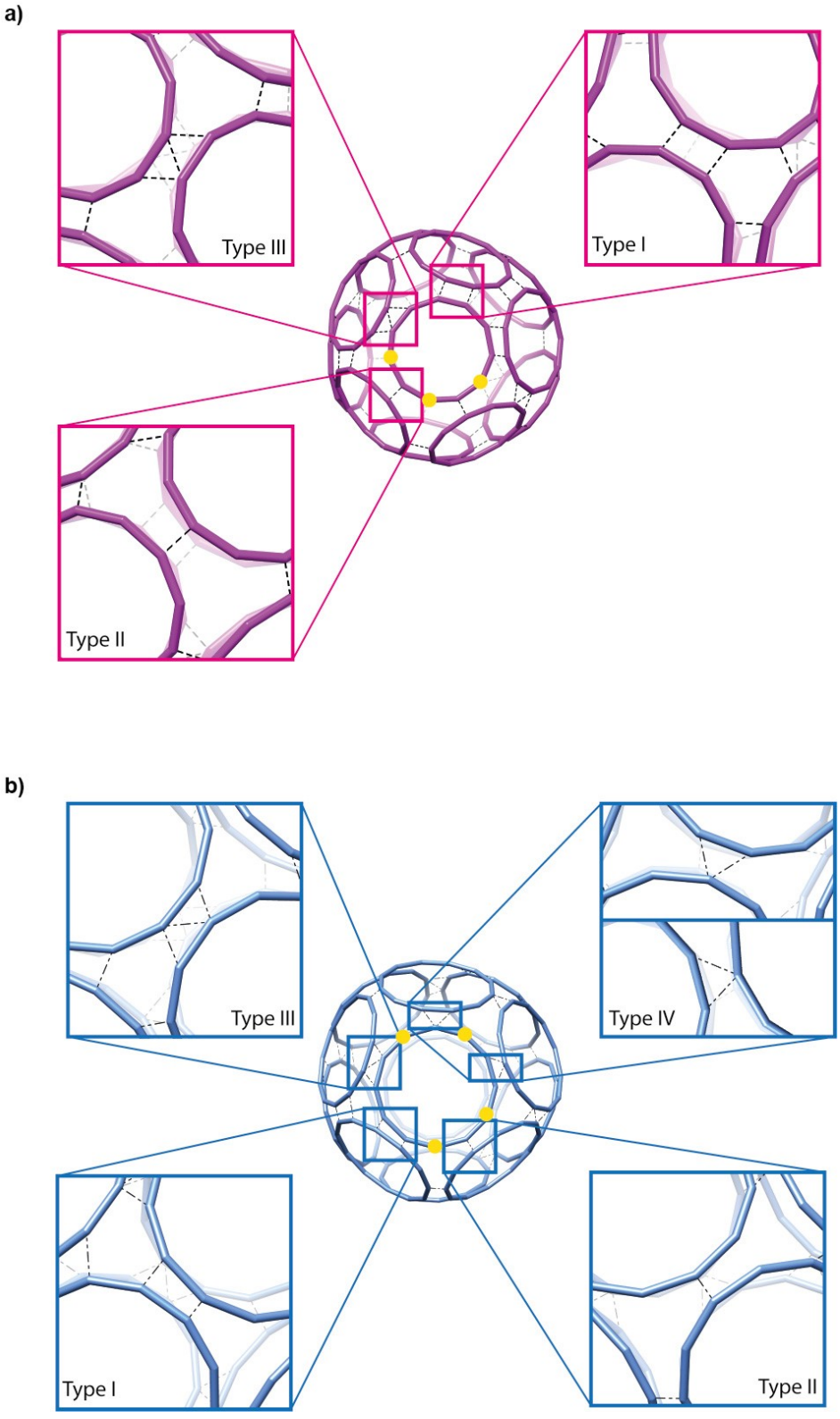

Fig. S6. Connection Maps between rings in TRAP-cages. Images are wireframe schematics showing cages made from **(a)**, 11mer rings and **(b)**, 12mer rings. Au(I)-mediated bonds between cysteines on opposing rings are indicated by dotted lines. In each case, in the central, representative ring, unbonded cysteines are indicated by a yellow circle.

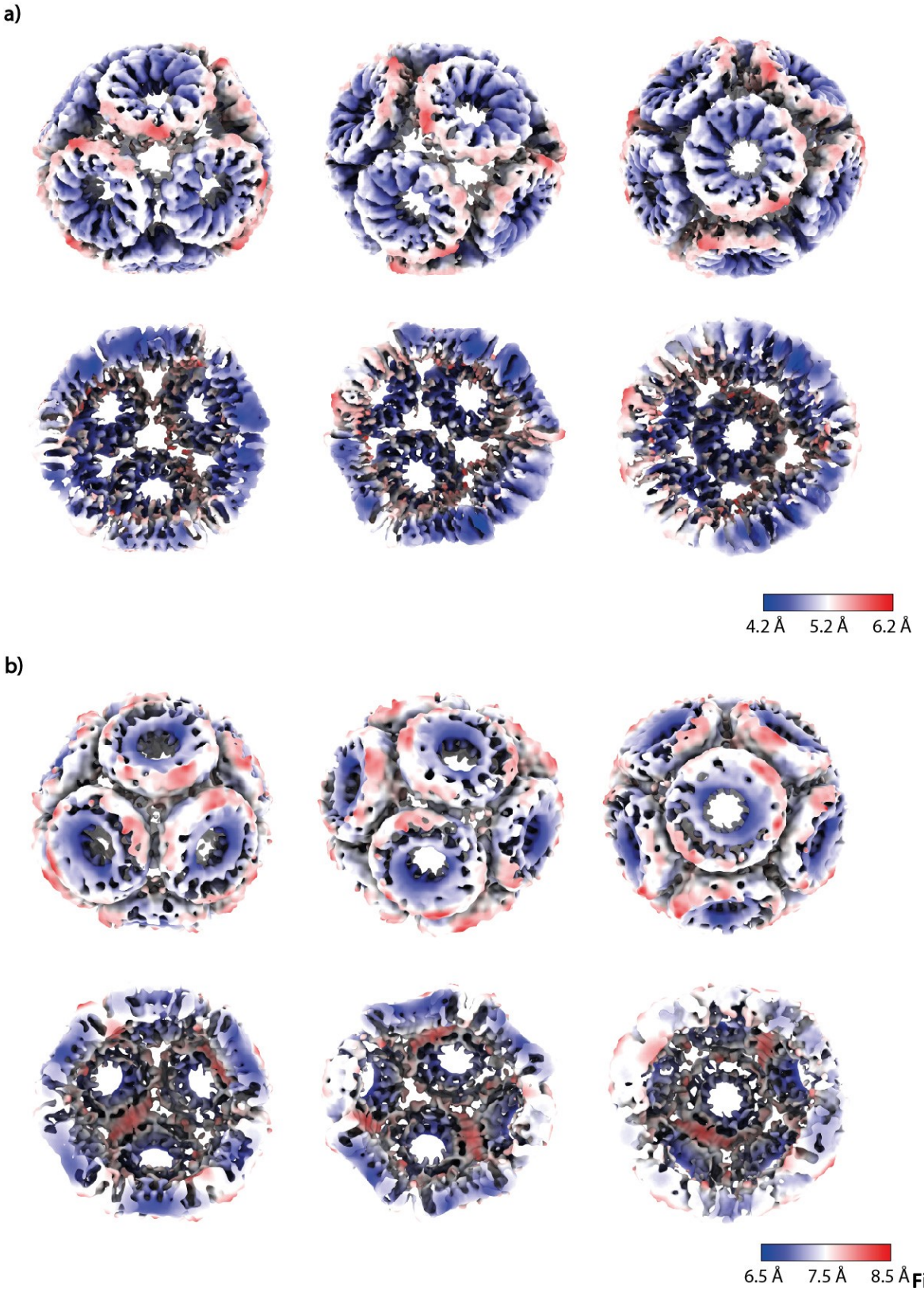

Fig. S7. Local resolution estimation of 12-ring TRAP-cages. (a), local resolution of $^{11}TRAP_{12}$ cage shown in three different views (top panel) together with respective cross-sections (bottom panel) and **(b)**, local resolution of $^{12}TRAP_{12}$ cage shown in three different views (top panel) together with respective cross-sections (bottom panel); scale bars showing the range of the resolution for each structure.

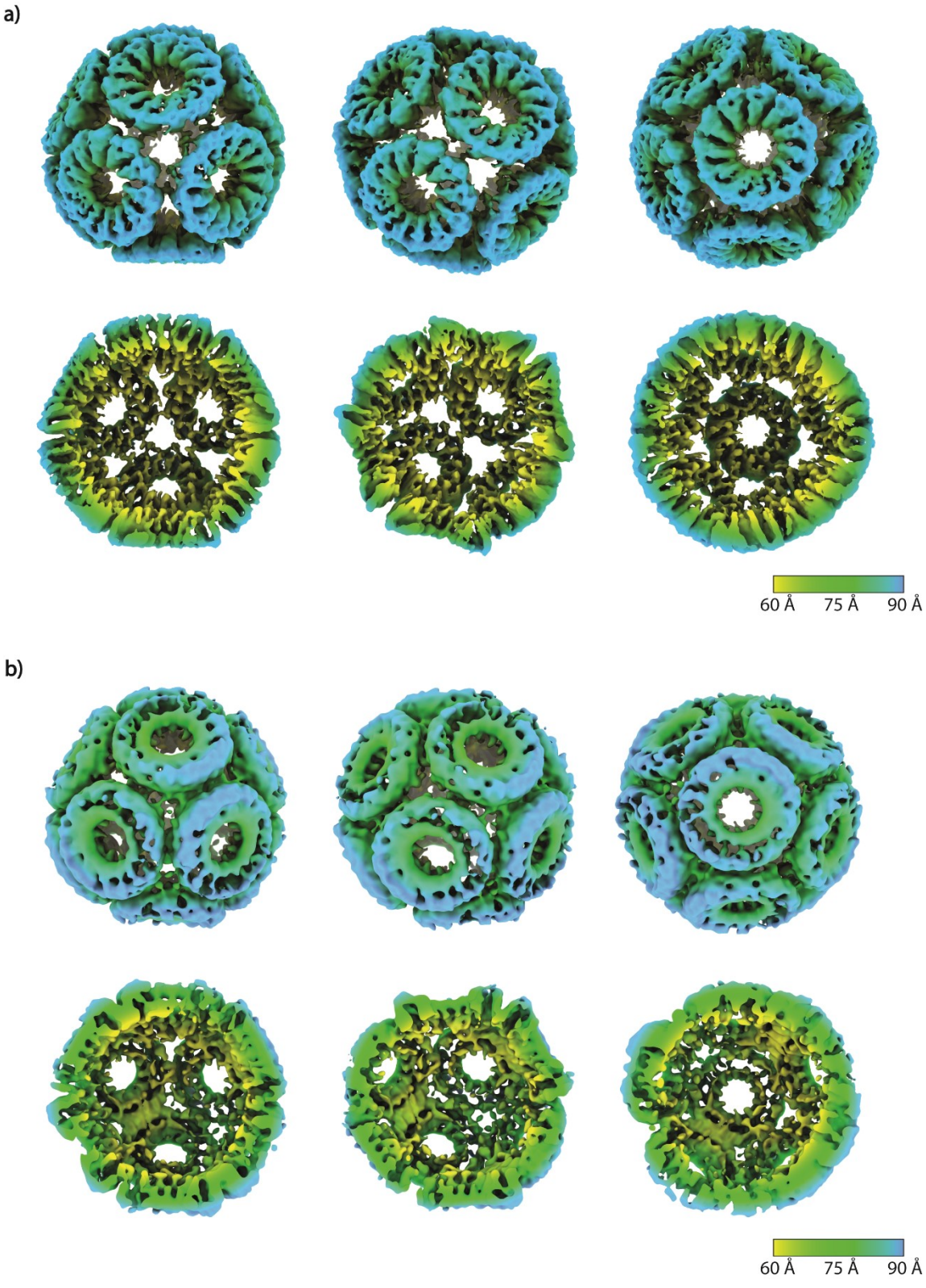

Fig. S8. Radius colouring of 12-ring TRAP cages. (a), radius coloured $^{11}TRAP_{12}$ cage shown in three different views (top panel) together with respective cross-sections (bottom panel) and **(b)**, radius coloured $^{12}TRAP_{12}$ cage shown in three different views (top panel) together with respective cross-sections (bottom panel); scale bars showing the range of the resolution for each structure.